Proceeding of the IEEE
International Conference on Robotics and Biomimetics
Dali, China, December 2019

# Ultrasound Image Filtering Using Partial Differential Equations *

**Jintao Ge, Yu Dai, Tong Chen, Jianxun Zhang, Xitong Yao**
*College of Artificial Intelligence, Nankai University*
daiyu@nankai.edu.cn

*Abstract* - **The speckle reducing anisotropic diffusion (SRAD) filter is extensively used to process the ultrasound image. However, in the image processed by SRAD filter, there could be slab effects, blurred weak boundaries, and lost details in the homogeneous region, and the iterative process cannot be terminated adaptively. To solve these problems, an improved diffusion coefficient is proposed, and the adaptive iterative termination condition is added. The result of the experiments shows that the optimization algorithm can efficiently eliminate the plate effect in the homogenous region and has a better visual effect than the traditional SRAD. And according to the criteria for quantifying algorithm performance, the optimization algorithm could not only well remove the speckle but also is more suitable for image segmentation than SRAD.**

***Index Terms - ultrasound imaging, adaptive iterative termination, anisotropic diffusion filter.***

## I. INTRODUCTION

Ultrasound images are widely used in the diagnosis of diseases such as kidney stones [1]. At the same time, due to the limitation of the ultrasonic imaging characteristic, the quality of the ultrasound images is poor, and there are usually a lot of speckle noises in the images [2, 3], which could affect the diagnosis of diseases, and also bring great challenges to the ultrasound images segmentation [4].

Several filtering algorithms have been proposed for the speckle reduction of ultrasound images [5]. The representative one is the Lee filter firstly proposed by Lee [6] in 1980. This filtering algorithm is based on local statistical properties, although it can suppress speckle noise well, it will make the boundary blurry and has weak detail retention [7, 8]. According to the adjustment of the gray level of the image, the diffusion filter is mainly divided into isotropic diffusion filter and Perona-Malik (PM) anisotropic diffusion filter [9]. In 2002, Yu [10] proposed a Speckle Reducing Anisotropic Diffusion (SRAD) filter for eliminating speckle noise of ultrasonic images, where the partial differential (PDE) method is used to remove scattered shifts. The SRAD filter combines the principle of local filtering based on Lee filter and PM anisotropic diffusion filter [11]. In the ultrasonic image with a large amount of speckle noise, compared with the traditional local statistical filter and anisotropic diffusion filter, the SRAD has better detail retention and edge enhancement [12, 13]. However, there are still many problems in the original SRAD filtering. For example, in the ultrasound image filtered by SRAD filter, there could be visually visible slab effects [14], which can't be eliminated easily [15]. At the same time, there are blurred weak boundaries and losses of image details in the filtered images, and the iterative process cannot be terminated adaptively. The occurrence of these defects would bring some interference to the doctor's clinical diagnosis and image segmentation [13].

Therefore, based on the original SRAD filtering, the following three optimizations are performed. (1)According to the characteristics of different regions of the image, a new diffusion coefficient is designed by using the idea of piecewise diffusion coefficient: the value of the diffusion coefficient in the homogenous image region is approximate to constant 1, ensuring the isotropic filtering effect of the image in the homogenous region while avoiding the generation of the slab effect; the fast attenuation in the image transition region improves the resolution of the image, which is beneficial to the preservation of the detail and the weak boundary; the value of the diffusion coefficient in the strong boundary region of the image is approximate to 0, conducive to sharpening strong boundaries. (2) In the diffusion coefficient, the scale control ratio of the homogenous region is set to be adjustable, which can solve the problem of different scale homogenous regions existing in the ultrasonic image, so that the new model can meet the application requirements in different situations. (3) The variable equivalent visual number is used to define adaptive iterative termination conditions [16].

The paper is organized as follows. In Section II, the traditional SRAD filter is introduced and discussed. Then, the improved SRAD filter is proposed in Section III. Since one of the direct aims of filtering is for image segmentation, the criteria for quantifying both the filtering performance of new SRAD and segmentation effect with the new filtering algorithm are proposed in Section □. In Section V, we conduct a lot of experiments with real ultrasound images to verify and discuss the proposed new filter.

## II. SPECKLE REDUCING ANISOTROPIC DIFFUSION (SRAD)

### A. SRAD

* This work is partially supported by National Key R&D Program of China (2017YFB1302803) and the Natural Science Foundation of Tianjin, China (18JCYBJC18800).



978-1-7281-6321-5/19//$31.00 ©2019 IEEE

For medical ultrasound images containing speckle, the image enhancement aims at removing the speckle without destroying important image features [17]. Therefore, Yu [10] proposed speckle suppression anisotropic diffusion filtering based on Lee filter and PM anisotropic diffusion filter. The nonlinear PDE for smoothing image is given by:

$$\begin{cases} \dfrac{\partial u(x,y,t)}{\partial t} = \operatorname{div}\{c[q(x,y,t)]\nabla u(x,y,t)\} \\ u(t=0) = u_0 \quad , \\ \dfrac{\partial u(x,y,t)}{\partial N} = 0 \quad , \quad u \in \partial\Omega \end{cases} \tag{1}$$

where $u(x,y,t)$ represents the initial image at time $t$, $x$ and $y$ represent the position of pixel point, $\nabla$ is the gradient operation, div is the divergence operator, and $\partial\Omega$ is the border of $\Omega$, $n$ denotes the outward unit normal vector, $u_0$ represents the initial image, $c(q(x,y,t))$ is the diffusion coefficient and given by

$$c(q(x,y,t)) = \frac{1}{1+\dfrac{q^2(x,y,t)-q_0^2(t)}{q_0^2(t)[1+q_0^2(t)]}}, \tag{2}$$

where $q(x,y,t)$ denotes the instantaneous coefficient of variation, determined by

$$q(x,y,t) = \sqrt{\frac{\frac{1}{2}(\frac{|\nabla u|}{u})^2 - \frac{1}{16}(\frac{\nabla^2 u}{u})^2}{[1+\frac{1}{4}(\frac{\nabla^2 u}{u})]^2}}, \tag{3}$$

where $q_0(t)$ denotes the speckle noise scale function, and the following formula is used to estimate $q_0(t)$:

$$q_0(t) \approx q_0 \exp(-\rho t), \tag{4}$$

where $\rho$ is a positive constant, $q_0$ is the speckle coefficient of variation in the observed image.

*B. SRAD's Defect*

Fig. 1(a) shows an original ultrasound image, Fig. 1(b) represents the region of interest (ROI) in the original ultrasound image and the corresponding result filtered by SRAD. It can be seen from Fig. 1(b) that after the image is filtered by SRAD, the plate effect appears in the homogeneous region [18], which constitutes false edge information, and the plate effect will always exist regardless of whatever parameters are taken by SRAD.

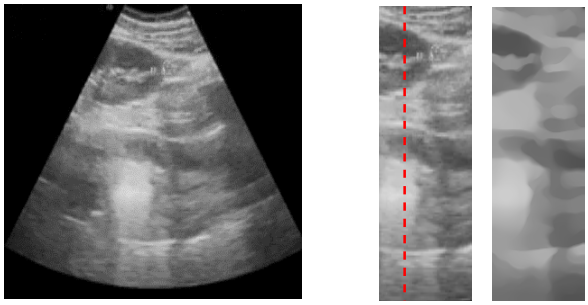

(a) Original ultrasound image (b) ROI and result filtered by SRAD

Fig. 1 Ultrasound image filtering experiments

Then the effect of the instantaneous coefficient of variation on the diffusion coefficient is qualitatively analyzed. To analyze SRAD filter further, the 50th column of the ROI is chosen as shown by the red dotted line in Fig. 1(b). In the chosen column, the gray value and instantaneous coefficient of variation corresponding to the pixel position from top to down are got as illustrated in Fig. 2(a) and Fig. 2(b) separately. Here $q_0$ is set to 0.01. Fig. 2(c) shows the relationship between the instantaneous coefficient of variation and the diffusion coefficient. In the homogeneous region of the image, the instantaneous coefficient varies little, but in the meantime, the diffusion coefficient changes obviously, which means that the diffusion coefficient is sensitive to the instantaneous coefficient. That is to say, the diffusion amplifies this change, which is the root cause of the plate effect in the uniform region of the image.

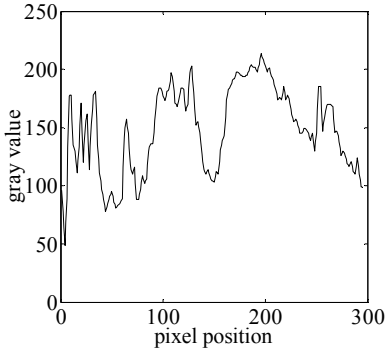


(a) The gray value in the profile

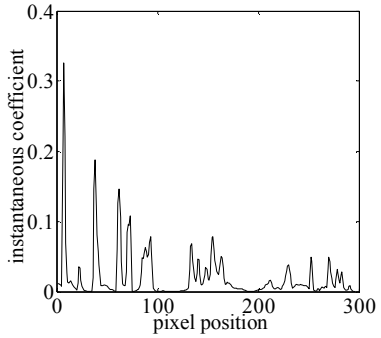


(b) The instantaneous coefficient of variation (ICOV)

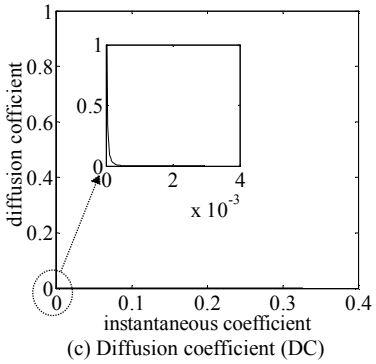


(c) Diffusion coefficient (DC)

Fig. 2 Analysis of diffusion coefficient

So it can be summarized that for an ideal diffusion coefficient, diffusion coefficient should change lightly in the homogenous region of the image, and is approximately equal

to isotropic diffusion; In the edge region of the image, the diffusion coefficient should be close to 0, thus playing the role of retaining details such as edges; In the transitional area of the image, the diffusion coefficient would quickly attenuate to shorten the processing time. To meet the above requirements, we propose a new diffusion coefficient as follows.

## III. NEW SRAD (NSRAD)

### A. New diffusion coefficient

The new diffusion coefficient is expressed as the following formula:

$$c(q)=\frac{\pi}{2}-\arctan\left\{k\left[q^2(x,y,t)-mq_0^2(t)\right]\right\}, \qquad (5)$$

where instantaneous coefficient of variation $q(x,y,t)$ and the speckle noise scale function $q_0(t)$ are still consistent with the original SRAD. $k$ is called the attenuation coefficient, it plays the role of controlling the decay rate of the diffusion coefficient, and $m$ is a constant called the homogenous region control ratio. In the filtering process, the filtering effect differs with the choice of different attenuation coefficients and homogenous region control ratios, so we could adjust m and k to meet the practical requirements. Fig. 3 below is a schematic diagram comparing the new diffusion coefficient with the original diffusion coefficient. Here, for the convenience of comparison, normalization is performed. The black curve and the red curve represent the original diffusion coefficient and the new diffusion coefficient separately.

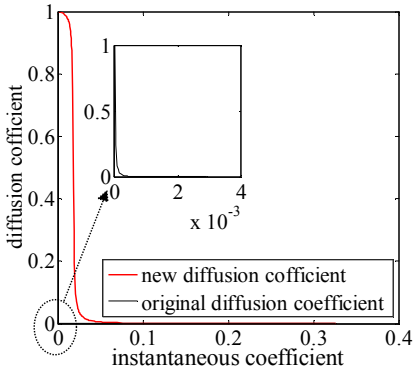


Fig. 3 Comparison of diffusion coefficients

As can be seen from Fig. 3, in the region where $q^2(x,y,t)$ is less than $mq_0^2(t)$, the change of the gradation is small, and the region is defined as a homogenous region. In the homogeneous region, the diffusion coefficient $c(q)$ approximately equals 1, which indicates that the diffusion velocities are approximately equal, and the new diffusion coefficient can make the isotropic diffusion similar in the homogeneous region. Moreover, the variation of the diffusion coefficient $c(q)$ in this segment is relatively slow compared to the original diffusion coefficient, so this design will well eliminate the plate effect caused by the extremely fast change of the diffusion coefficient when the original SRAD filtering is performed in the homogeneous region of the image. The region where $q^2(x,y,t)$ is approximately equal to $mq_0^2(t)$ corresponds to the transitional region such as texture and weak boundary of the image, and the diffusion coefficient decays rapidly. This indicates that the diffusion coefficient is sensitive to the change of the instantaneous coefficient of variation. When the instantaneous coefficient of variation changes greatly, the coefficients will have a larger change. This will improve the capability to maintain texture details and weak boundaries. The area where $q^2(x,y,t)$ is bigger than $mq_0^2(t)$ corresponds to the edge of the image, the transient coefficient of variation is relatively large, and the diffusion coefficient is small and close to zero, which affects on preserving the edge.

### B. Adaptive iterative termination condition

The number of iterations of the original SRAD requires to be set artificially. Different iterations are needed for different images and the number of iterations cannot be adjusted adaptively. If the number of iterations is too large, the edge of the image will be blurred; if the number of iterations is small, the effect of noise reduction is not obvious enough. $E_n$ is one of the evaluation indicators of the filtering, and is expressed by the following formula:

$$E_n=\frac{\mu^2}{\sigma^2}, \qquad (6)$$

where $\mu$ and $\sigma$ respectively represent the mean and standard deviation of the image after the filtering. As the number of iterations increases, the intensity of speckle-noise gradually decreases, and the value of $E_n$ increases. Fig. 4 shows the relationship between $E_n$ and Iteration number.

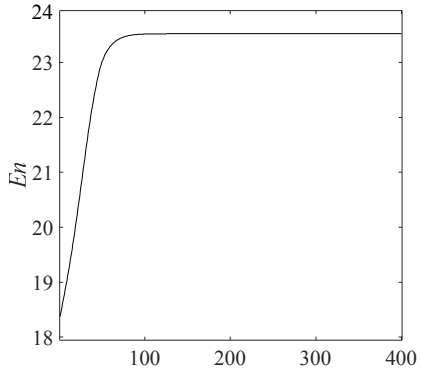


Fig. 4 $E_n$ figure

As shown in Fig. 4, $E_n$ varies little after 100 iterations. Therefore, an adaptive iterative termination condition is designed, which could make the program break out of the loop when the relative change of $E_n$ in the image filtering process is lower than a certain threshold [19]. This condition is shown as follows:

$$R_e=\left|\frac{E_t-E_{t-\Delta t}}{E_{t-\Delta t}}\right|\le\varepsilon, \qquad (7)$$

where $R_e$ is defined as the relative effective number of looks increment, $\Delta t$ is time step, $E_t$ represents $E_n$ at time $t$, and $E_{t-\Delta t}$ represents $E_n$ at the previous moment. $\varepsilon$ is a small constant. It is proved by experiments that when the $\varepsilon$ equals 0.0001, good filtering and detail retention capability can be ensured, and the filtering processing speed is improved.

### C. Discretization of NSRAD

The nonlinear PDE of NSRAD for smoothing image is given as follows:

$$\begin{cases} \dfrac{\partial u}{\partial t} = \operatorname{div}[c_N(q)\nabla u(x,y,t)] \\ u_0 = g \quad . \\ \dfrac{\partial u}{\partial N} = 0 \quad , \quad u \in \partial\Omega \end{cases} \tag{8}$$

In (8), to distinguish from the continuous diffusion coefficient, a new diffusion coefficient is written as $c_N(q)$. The differential equation may be solved numerically using the Jacobi method [10]. The mesh size is $h$ in the $x$ and $y$ directions.

Time and space coordinates are discretized as follows:

$$t = n\Delta t, n = 0,1,2,..., \tag{9}$$

$$x = ih, i = 0,1,2,...,M-1; y = jh, j = 0,1,2,...,N-1, \tag{10}$$

where $Mh \times Nh$ is the size of the image.

Let

$$u_{i,j}^n = u(ih, ih, n\Delta t). \tag{11}$$

Then a three-stage approach is used to calculate the NSRAD PDE. Firstly, the derivative is calculated, where the right gradient at time t is calculated as:

$$\nabla_R u_{i,j}^n = \left(\frac{u_{i+1,j}^n - u_{i,j}^n}{h}, \frac{u_{i,j+1}^n - u_{i,j}^n}{h}\right), \tag{12}$$

the left gradient at time $t$ is calculated as:

$$\nabla_L u_{i,j}^n = \left(\frac{u_{i,j}^n - u_{i-1,j}^n}{h}, \frac{u_{i,j}^n - u_{i,j-1}^n}{h}\right), \tag{13}$$

and the central standard gradient at time $t$ is calculated as:

$$\nabla^2 u_{i,j}^n = \frac{u_{i+1,j}^n + u_{i-1,j}^n + u_{i,j+1}^n + u_{i,j-1}^n - 4u_{i,j}^n}{h^2}, \tag{14}$$

with the symmetric boundary conditions:

$$u_{-1,j}^n = u_{0,j}^n, u_{M,j}^n = u_{M-1,j}^n, j = 0,1,2,...,N-1, \tag{15}$$

$$u_{i,-1}^n = u_{i,0}^n, u_{i,N}^n = u_{i,N-1}^n, j = 0,1,2,...,M-1. \tag{16}$$

Secondly, the diffusion coefficient $C_N(q)$ is calculated as:

$$c_{i,j}^n(q) = \frac{\pi}{2} - \arctan[k(q^2(x,y,t) - mq_0^2(t)], \tag{17}$$

where $q(x,y,t)$ denotes the instantaneous coefficient of variation determined by

$$q_{i,j}^n = \sqrt{\frac{(\frac{1}{2})(\frac{|\nabla u_{i,j}^n|}{u_{i,j}^n})^2 - (\frac{1}{16})(\frac{\nabla^2 u_{i,j}^n}{u_{i,j}^n})^2}{[1 + (\frac{1}{4})(\frac{\nabla^2 u_{i,j}^n}{u_{i,j}^n})]^2}}. \tag{18}$$

Moreover, the divergence of $c(\cdot)\nabla u$ needed for SRAD PDE is calculated by:

$$d_{i,j}^n = \frac{1}{h^2}[c_{i+1,j}^n(u_{i+1,j}^n - u_{i,j}^n) + c_{i,j}^n(u_{i-1,j}^n - u_{i,j}^n) + c_{i,j+1}^n(u_{i,j+1}^n - u_{i,j}^n) + c_{i,j}^n(u_{i,j-1}^n - u_{i,j}^n)], \tag{19}$$

with symmetric boundary conditions:

$$d_{-1,j}^n = d_{0,j}^n, d_{M,j}^n = d_{M-1,j}^n, j = 0,1,2,...,N-1, \tag{20}$$

$$d_{i,-1}^n = d_{i,0}^n, d_{i,N}^n = d_{i,M-1}^n, j = 0,1,2,...,M-1. \tag{21}$$

Finally, by assuming time derivative with forward difference, the PDE of the formula can be given by:

$$u_{i,j}^{n+1} = u_{i,j}^n + \frac{1}{4}\Delta t d_{i,j}^n, \tag{22}$$

which is called the NSRAD update function.

## IV. Criteria for Quantifying

### A. Criteria for quantifying to remove the speckle

To compare the speckle removing performances with different speckle reduction schemes, the following indicators are adopted: effective number of looks ($E_n$) and speckle index ($S_i$) [12].

$E_n$ is used to indicate the relative intensity of image speckle noise. It is defined by (6). The larger $E_n$ is, the better the speckle of the algorithm is removed.

The definition of the $S_i$ is similar to the $E_n$, which is normalized by solving the ratio of the standard deviation and the mean of the image. It is defined by

$$S_i = \frac{1}{M \times N}\sum_{i=1}^{M}\sum_{j=1}^{N}\frac{\sigma_{i,j}}{\mu_{i,j}}. \tag{23}$$

The smaller the value of $S_i$ is, the better the speckle effect of the algorithm is removed.

### B. Criteria for quantifying segmentation

To evaluate the improvement of the segmentation effect by the optimized NSRAD filtering algorithm, the edge-based Hausdorff distance ($D_h$) and the mean absolute distance ($D_m$) are chosen to measure the distance difference between the contour segmented by algorithm and the contour defined by the doctor.

$D_h$ is defined by

$$D_h = \max d\left[Q, P(x_j)\right] \quad , \quad j \in [1, J]. \tag{24}$$

$D_m$ is defined by

$$D_m = \frac{1}{J}\sum_{j=1}^{J} d\left[Q, P(x_j)\right] \quad , \quad j \in [1, J], \tag{25}$$

$$d\left[Q, P(x)\right] = \min\left(\|y - x\|\right) \quad , \quad y \in Q, \tag{26}$$

Where $Q$ represents the contour defined by doctor and $P$ represents the contour segmented by algorithm, and $J$ is the total number of pixels on the contour segmented by contour. $D_h$ represents the furthest distance within matching points in the two contours. $D_m$ represents the average distance between the two contours. The closer $D_h$ and $D_m$ are to 0, the closer the contour obtained by the algorithm is to the true contour.

## V. Results and Discussion

In this section, both NSRAD and SRAD filters are tested using 20 sets of real ultrasound images. The experimental software environment is matlab2015b, using 64-bit Windows7 operating system; The hardware environment is Intel (R) Core (TM) i5-4590 CPU 3.30GHZ, RAM: 8.00GB. The kidney

ultrasound images used in the experiment are from the First Affiliated Hospital of the People's Liberation Army General Hospital (304). The ultrasonic machine used for ultrasonic image acquisition is the Apogee 1000 ultrasonic diagnostic system produced by Shantou Ultrasonic Instrument Research Institute Co., Ltd. In the experiment, the time step is set to 0.05 s, and the number of iterations is set to 400. In the experiment, $k$ is set equal to 30 and $m$ to 0.5. The other main parameters of SRAD are set according to [6].

### A. *Denoising result*

Fig. 5(a) is an image filtered by the original SRAD and Fig. 5(b) is an image filtered by NSRAD. Table I summarizes the speckle removal performance.

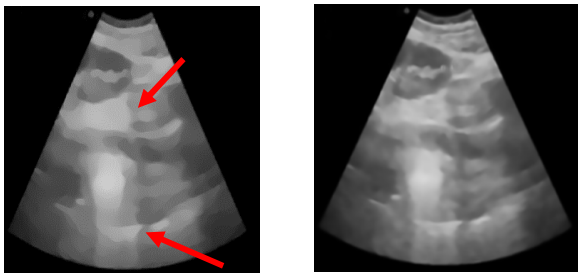

(a) Image filtered by SRAD (b) Image filtered by NSRAD

Fig. 5 Ultrasound image filtering results

From Fig. 5(a) and Fig. 1(b), it can be seen that the plate effect is very obvious in the SRAD filtering of real ultrasound images. The false boundary generated by the plate effect could have an adverse effect on the subsequent segmentation. For real ultrasound images, it can be seen from Fig. 5(b) and Table I that the optimized filtering algorithm not only has a good visual effect but also improves the speckle removal performance.

TABLE I

CRITERIA FOR QUANTIFYING TO REMOVE THE SPECKLE

| Filter | Speckle noise removal | |
|---|---|---|
| | $E_n$ | $S_i$ |
| Fig. 1(a) | 18.81 ± 1.32 | $1.29^{-5} \pm 8.17^{-12}$ |
| Median | 19.12 ± 1.40 | $1.28^{-5} \pm 8.05^{-12}$ |
| Mean | 19.28 ± 1.44 | $1.27^{-5} \pm 8.01^{-12}$ |
| Wavelet | 20.24 ± 1.71 | $1.24^{-5} \pm 7.52^{-12}$ |
| Non Local Mean | 19.69 ± 1.55 | $1.26^{-5} \pm 7.87^{-12}$ |
| Lee | 19.01 ± 1.36 | $1.28^{-5} \pm 8.22^{-12}$ |
| PM | 20.85 ± 1.89 | $1.23^{-5} \pm 7.47^{-12}$ |
| SRAD | 22.58 ± 2.49 | $1.18^{-5} \pm 6.84^{-12}$ |
| NSRAD | 23.08 ± 2.65 | $1.17^{-5} \pm 6.76^{-12}$ |

### B. *Real ultrasound image segmentation Results*

Fig. 6 shows the companion of segmentation results when Distance Regularized Level Set Evolution [20] is applied under different flitering algorithms are used. The blue curve in Fig. 6 represents the initial contour, the yellow curve represents the segmentation results with SRAD filter and NSRAD filter, and the red curve represents the segmentation result defined by the doctor.

Table  summarizes the segmentation results of DRLSE when SRAD and NSRAD filter are separately used. The experimental data are expressed as mean ± variance. As can be seen from Table  and Fig. 6, NSRAD can improve the accuracy of segmentation compared to SRAD, and the $D_h$ is reduced by 32.768%, and the $D_m$ is reduced by 27.064%.

TABLE 

Criteria for quantifying to remove the speckle

| Filter | Image segmentation | |
|---|---|---|
| | $D_h$ | $D_m$ |
| SRAD | 16.82 ± 13.96 | 5.20 ± 0.67 |
| NSRAD | 11.31 ± 2.06 | 3.79 ± 0.65 |

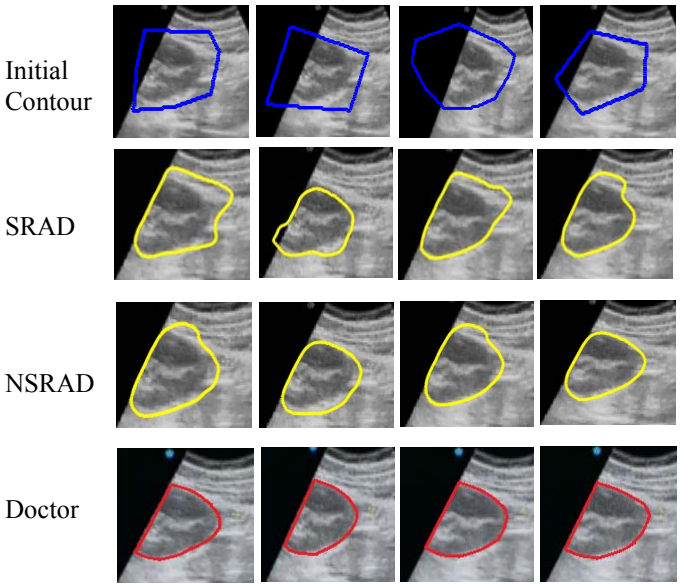


Fig. 6 Image segmentation results under different filters

## . CONCLUSIONS

In this paper, a new diffusion coefficient has been proposed in the framework of the SRAD filter, and the adaptive iterative termination condition is defined. The experiment results show that NSRAD can eliminate the plate effect that occurs in the homogeneous region of the original SRAD and enhance the sensitivity of the diffusion coefficient in the transitional area. The results also show that both visual effects and the capability to maintain boundaries and details are improved. At the same time, the new model can improve the accuracy of image segmentation.

Our futuer work will mainly focus on the selection of some key coefficients of the filter. Besides that, we will collect more data and do more experiments to verify and improve the proposed filter.

## REFERENCES

[1] R. Dass, "Speckle Noise Reduction of Ultrasound Images Using BFO Cascaded with Wiener Filter and Discrete Wavelet Transform in Homomorphic Region," *Procedia Computer Science,* vol. 132, pp. 1543-1551, 2018/01/01/ 2018.

[2] A. F. de Araujo, C. E. Constantinou, and J. M. R. S. Tavares, "Smoothing of ultrasound images using a new selective average filter," *Expert Systems with Applications,* vol. 60, pp. 96-106, 2016/10/30/ 2016.

[3] P. V. Sudeep *et al.*, "Speckle reduction in medical ultrasound images using an unbiased non-local means method," *Biomedical Signal Processing and Control,* vol. 28, pp. 1-8, 2016/07/01/ 2016.

[4] J. Zhang, G. Lin, L. Wu, and Y. Cheng, "Speckle filtering of medical ultrasonic images using wavelet and guided filter," *Ultrasonics,* vol. 65, pp. 177-193, 2016/02/01/ 2016.

[5] I. Elyasi, M. A. Pourmina, and M.-S. Moin, "Speckle reduction in breast cancer ultrasound images by using homogeneity modified bayes shrink," *Measurement,* vol. 91, pp. 55-65, 2016/09/01/ 2016.
[6] J.-S. Lee, "Speckle analysis and smoothing of synthetic aperture radar images," *Computer Graphics and Image Processing,* vol. 17, no. 1, pp. 24-32, 1981/09/01/ 1981.
[7] I. Elyasi and M. A. Pourmina, "Reduction of speckle noise ultrasound images based on TV regularization and modified bayes shrink techniques," *Optik,* vol. 127, no. 24, pp. 11732-11744, 2016/12/01/ 2016.
[8] P. V. Sudeep *et al.*, "Enhancement and bias removal of optical coherence tomography images: An iterative approach with adaptive bilateral filtering," *Computers in Biology and Medicine,* vol. 71, pp. 97-107, 2016/04/01/ 2016.
[9] P. Perona and J. Malik, "Scale-space and edge detection using anisotropic diffusion," *IEEE Transactions on Pattern Analysis and Machine Intelligence,* vol. 12, no. 7, pp. 629-639, 1990.
[10] Y. Yongjian and S. T. Acton, "Speckle reducing anisotropic diffusion," *IEEE Transactions on Image Processing,* vol. 11, no. 11, pp. 1260-1270, 2002.
[11] L. Zheng and K. Tian, "Center affine filter based adaptive image despeckling method with preserving details," *Applied Acoustics,* vol. 155, pp. 16-23, 2019/12/01/ 2019.
[12] M. Ben Abdallah, J. Malek, A. T. Azar, H. Belmabrouk, J. Esclarín Monreal, and K. Krissian, "Adaptive noise-reducing anisotropic diffusion filter," *Neural Computing and Applications,* journal article vol. 27, no. 5, pp. 1273-1300, July 01 2016.
[13] K. Singh, S. K. Ranade, and C. Singh, "A hybrid algorithm for speckle noise reduction of ultrasound images," *Computer Methods and Programs in Biomedicine,* vol. 148, pp. 55-69, 2017/09/01/ 2017.
[14] D. Koundal, S. Gupta, and S. Singh, "Neutrosophic Based Nakagami Total Variation Method for Speckle Suppression in Thyroid Ultrasound Images," *IRBM,* vol. 39, no. 1, pp. 43-53, 2018/02/01/ 2018.
[15] J. Bai and X.-C. Feng, "Image Denoising Using Generalized Anisotropic Diffusion," *Journal of Mathematical Imaging and Vision,* journal article vol. 60, no. 7, pp. 994-1007, September 01 2018.
[16] H. Talebi, X. Zhu, and P. Milanfar, "How to SAIF-ly Boost Denoising Performance," *IEEE Transactions on Image Processing,* vol. 22, no. 4, pp. 1470-1485, 2013.
[17] B. Ni, F. He, and Z. Yuan, "Segmentation of uterine fibroid ultrasound images using a dynamic statistical shape model in HIFU therapy," *Computerized Medical Imaging and Graphics,* vol. 46, pp. 302-314, 2015.
[18] J.-J. Mei, T.-Z. Huang, S. Wang, and X.-L. Zhao, "Second order total generalized variation for speckle reduction in ultrasound images," *Journal of the Franklin Institute,* vol. 355, no. 1, pp. 574-595, 2018/01/01/ 2018.
[19] S. Peng, W. Ser, B. Chen, L. Sun, and Z. Lin, "Robust Constrained Adaptive Filtering Under Minimum Error Entropy Criterion," *IEEE Transactions on Circuits and Systems II: Express Briefs,* vol. 65, no. 8, pp. 1119-1123, 2018.
[20] Li C, Xu C, Gui C, et al. “Distance Regularized Level Set Evolution and Its Application to Image Segmentation”. *IEEE Transactions on Image Processing*, 2010, 19(12):3243-3254.